(*The 40th International Workshop on Water Waves and Floating Bodies, May 2025, Shanghai, China*)

On natural modes in the dock of a ship

Mingxuan Li[1]*, Xinshu Zhang[1], Bernard Molin[2], Robert F. Beck[3]

[1] State Key Laboratory of Ocean Engineering, Shanghai Jiao Tong University, Shanghai 200240, China

[2] Ecole Centrale Marseille & IRPHE

[3] University of Michigan, Ann Arbor, MI 48109, USA

Highlights

- A new simplified model is proposed to predict the natural frequencies and modal shapes of a ship's dock, with comprehensive comparisons conducted against numerical results from WAMIT.
- The accuracy of the proposed model is further verified through a series of parametric analyses.

1 Introduction

The dock is designed to accommodate various types of boats and to facilitate their launch and recovery. When the frequency of incident waves aligns with the dock's natural frequency, resonant fluid motion can occur, similar to the sloshing phenomenon observed in moonpools. During resonances, the free-surface response can increase significantly, potentially leading to collisions or even capsizing of the boats. Therefore, accurate prediction of the natural frequencies of the dock is crucial.

To simplify computations, the numerical model can be appropriately reduced, for example, assuming that the ship is fixed. Bass *et al.* (2004) combined commercial CFD code with a ship-motion prediction program to first compute the surface elevation inside the dock of a Landing Platform Dock (LPD), and then analyze the natural frequencies. Cartwright *et al.* (2007) conducted numerical simulations of a two-dimensional LPD model with a dock using the Smoothed Particle Hydrodynamics (SPH) method, analyzing the influence of dock design parameters on the free-surface response and comparing the numerical results with the experimental data. However, few studies have focused on estimating the natural periods of a dock on a ship.

This paper presents a theoretical model for rapid estimation of the natural frequencies of a dock on a ship. In addition, the wave diffraction/radiation code WAMIT was employed to compute the free-surface response. The accuracy of the proposed model was validated by comparing the resonance frequencies and modal shapes with the WAMIT results. An investigation of the natural modes identified the presence of short-wave components in the longitudinal direction within the dock, which can be explained by the fact that several natural frequencies are close to each other.

2 Theoretical Analysis

The sketch of a ship with a dock and the coordinate system is shown in Fig. 1. We focus on the resonant free-surface response inside the dock. The velocity potential is supposed to be harmonic in time such that $\Phi(x, y, z, t) = \phi(x, y, z)e^{-\mathrm{i}\omega t}$, where $\phi(x, y, z)$ is the spatial velocity potential.

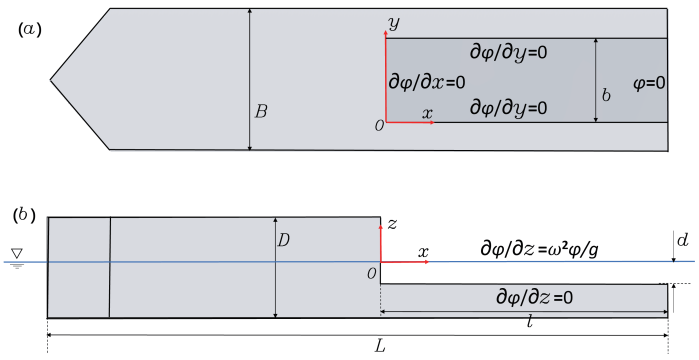

Figure 1: Sketch of the ship and boundary conditions. (a): top view; (b): side view.

*Presenting author

The governing equation within the fluid domain inside the dock can be written as:

$$\Delta\phi = 0, \tag{1}$$

where Δ is the Laplace operator. The boundary conditions are denoted in the sketch. The key boundary condition is $\phi = 0$ at the opening of the dock, which works well for a moonpool problem (Molin *et al.*, 2018; Zhang *et al.*, 2019).

Based on the boundary conditions, the natural modes can be written as:

$$\Phi(x, y, z, t) = \cos(\lambda_m x)\cos(\mu_n y)\cosh(k_{mn}(z + d))\cos(\omega_{mn} t), \tag{2}$$

with

$$\lambda_m = (2m - 1)\pi/2l, \quad \mu_n = n\pi/b, \quad k_{mn} = \sqrt{\lambda_m^2 + \mu_n^2}, \tag{3}$$

where l and b are the length and width of the dock, respectively. $m = 1, 2, 3, \cdots$ and $n = 0, 1, 2, \cdots$. Thus, the natural frequencies can be computed by:

$$\omega_{mn}^2 = g k_{mn} \tanh k_{mn} d, \tag{4}$$

where d is the water depth in the dock.

3 Numerical Model

The numerical model is built based on the parameters described in Hopman *et al.* (1994). As the model in that paper provides limited details, certain simplifications are made when building up the test model. The operational draft of the dock is determined according to Wang *et al.* (2023).

The length at the waterline of the ship is $L = 160$ m. The beam is $B = 22.6$ m, and the draft is $D = 5.44$ m. The length of the dock is $l = 73$ m, and the width is $b = 13.4$ m. The water depth inside the dock is $d = 1.93$ m. The dock is assumed to be flat and it has no camber.

An array of numerical wave gauges (NWGs) was placed within the dock, ensuring that at least 20 NWGs covered one full wavelength. WAMIT was adopted to compute the free-surface elevation inside the dock under fixed conditions. Through convergence analysis, it was determined that the computational model contains around 4000 panels.

4 Results

The simulations were performed for three wave directions: following sea, beam sea, and quartering sea. Surface elevations were plotted at selected NWGs, with the peaks corresponding to the natural frequencies of each mode. Given the small surface elevation amplitude at higher-order resonances, only the first few resonance modes are analyzed. The simulation results are shown in Table 1. It is evident that the natural frequencies obtained using WAMIT are in very good agreement with the predicted values.

Natural frequencies	ω_{10}	ω_{20}	ω_{30}	ω_{40}	ω_{50}
Prediction (rad s^{-1})	0.094	0.280	0.465	0.646	0.824
WAMIT (rad s^{-1})	0.090	0.270	0.450	0.625	0.795
Natural frequencies	ω_{11}	ω_{21}	ω_{31}		
Prediction (rad s^{-1})	0.991	1.021	1.079		
WAMIT (rad s^{-1})	1.000	1.028	1.083		
Natural frequencies	ω_{12}	ω_{22}	ω_{32}		
Prediction (rad s^{-1})	1.820	1.832	1.856		
WAMIT (rad s^{-1})	1.821	1.833	1.855		

Table 1: Natural frequencies predicted by the present model and WAMIT.

In following sea, the free-surface response at NWG1 is shown in Fig. 2, where A is the amplitude of the incident wave. Fig. 3 shows the modal shape of the sloshing modes and compares them with the WAMIT solutions, showing excellent agreement.

Fig. 4 presents the free-surface response amplitude with respect to wave frequency at NWG1 in beam sea. Fig. 5 compares the modal shapes predicted by the theoretical model with those obtained using WAMIT at the peak frequencies shown in Fig. 4. Considering that those modal shapes are very similar, it is clear that the predicted natural frequencies match well with the WAMIT results, particularly for values of n greater than 1.

As can be seen in Table 1, the values of ω_{mn} are very close when $n = 1$, and this phenomenon becomes more pronounced as n increases. As shown in Fig. 5, for $m = 2$, the peaks of the free-surface elevation along

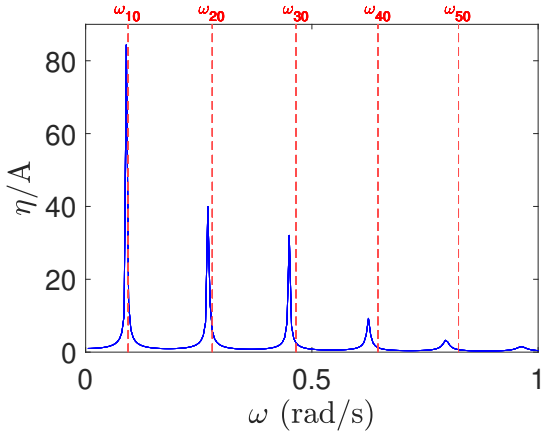

Figure 2: Free-surface response of NWG1 (0.1 m, 6.6 m, 0) computed by WAMIT in following sea. The red dashed lines indicate the natural frequencies.

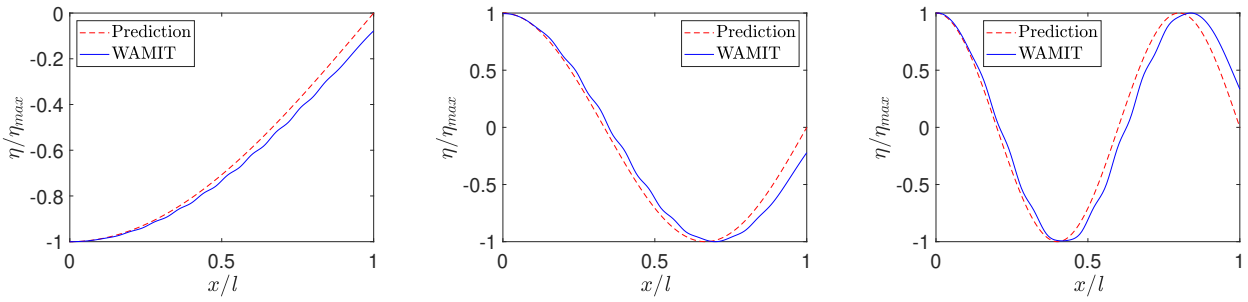

Figure 3: Natural modes of free surface in following sea for n=0. (a): m=1. (b): m=2. (c): m=3. η_{max} is the maximum value of the free-surface response.

the longitudinal direction occur at $x = 0$ and $x = \frac{2}{3}l$. For $m = 3$, the peaks of the free-surface elevation along the longitudinal direction are located at $x = 0$, $x = 0.4l$, and $x = 0.8l$, which is consistent with theoretical predictions. However, as illustrated in Fig. 5(a) and (e), a subtle fluctuation is evident in the plot of the modal shapes. This observed fluctuation may be attributed to an insufficient frequency resolution to capture the exact natural frequencies. Specifically, when the transverse resonance is of high order, the variation in the natural frequencies with respect to m becomes very small. As a result, even minor deviation from the natural frequencies can cause the overlapping of resonance modes of different orders, which manifests as slight fluctuations in the modal shapes.

Parametric studies have been conducted, with Fig. 6 showing a comparison between the predicted values of ω_{11} and the simulation results as the main dimensions of the dock are varied. It is observed that an increase in the depth of the dock leads to higher natural frequencies, whereas an increase in the width of the dock results in lower natural frequencies. Although the predicted values are slightly lower than those computed by WAMIT across the range of dimensions, there is still a strong agreement between the two, further validating the accuracy of the prediction method. In future study, the reliability of the prediction method can be further validated through experiments conducted in an ocean wave basin.

Acknowledgement

The present work is sponsored by the National Natural Science Foundation of China under Grant No. 52171269.

References

Bass, D, Molyneux, D & McTaggart, K. 2004 Simulating wave action in the well deck of landing platform dock ships using computational fluid dynamics. In *Warship 2004*, London, England.

Cartwright, B, Renilson, G, Macfarlane, G *et al.* 2007 Motions of a landing craft in a flooded well-dock effect of well dock design. In *International Conference on Military Support Ships*, London, England.

Hopman, H, Kapsenberg, G, K & Krikke, E, M. 1994 Design and hydromechanic aspects of the amphibious transport vessel for the royal netherlands navy. *Naval Engineers Journal* **106** (3), 163–174.

Molin, B, Zhang, X, Huang, H & others. 2018 On natural modes in moonpools and gaps in finite depth. *Journal of Fluid Mechanics* **840**, 530–554.

Wang, Z, You, Y & Feng, A. 2023 Investigation on the wave characteristic inside the well dock of LPD ship in open ocean. In *Proceedings of the 33rd International Ocean and Polar Engineering Conference*, ISOPE-I-23-322. Ottawa, Canada.

Zhang, X, Huang, H & Song, X. 2019 On natural frequencies and modal shapes in two-dimensional asymmetric and symmetric moonpools in finite water depth. *Applied Ocean Research* **82**, 117–129.

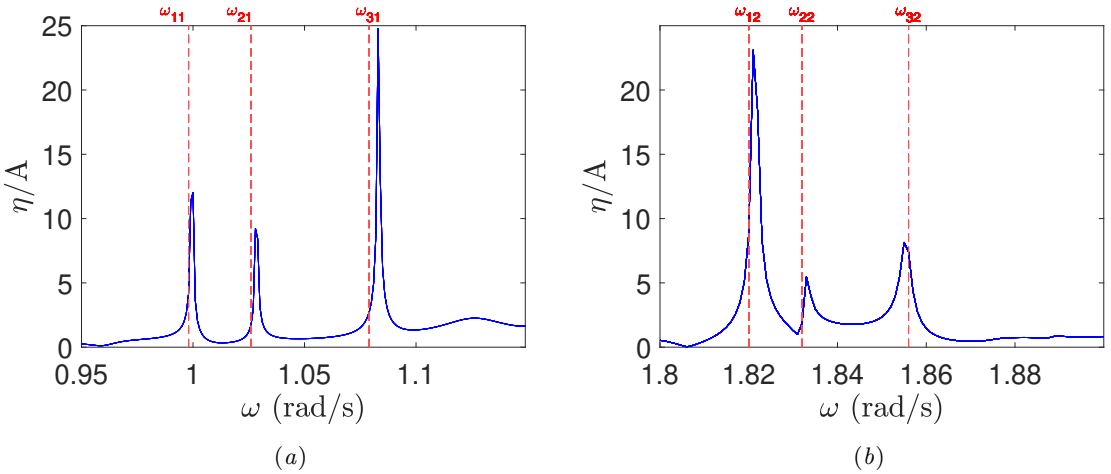

Figure 4: Free-surface response of NWG1 computed by WAMIT in beam sea at frequencies near ω_{m1} (a) and ω_{m2} (b). Red dashed lines denote the natural frequencies.

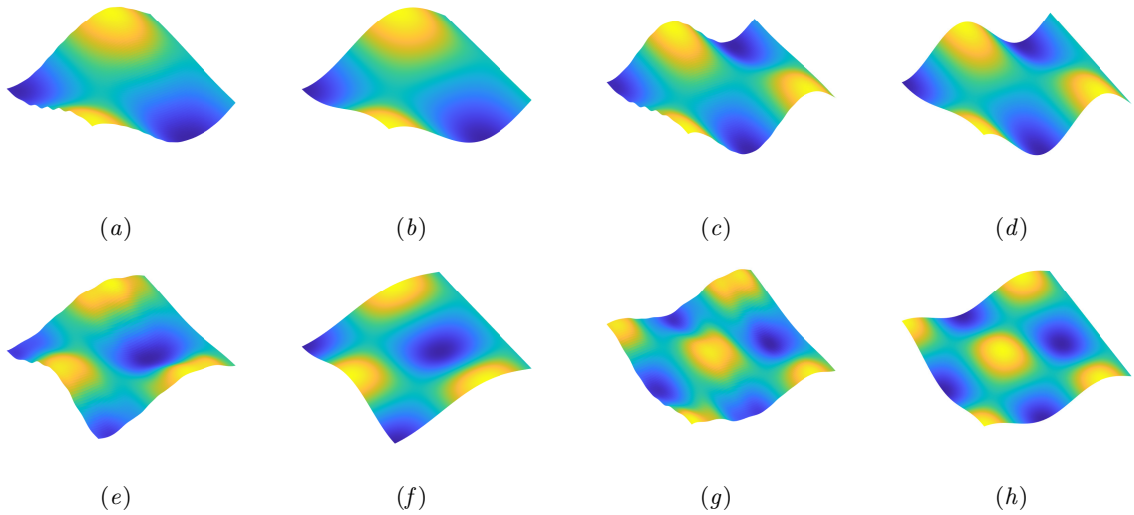

Figure 5: Natural modes of the dock in beam sea. (a): WAMIT results for ω_{21}; (b): Present model for ω_{21}; (c): WAMIT results for ω_{31}; (d): Present model for ω_{31}; (e): WAMIT results for ω_{22}; (f): Present model for ω_{22}; (g): WAMIT results for ω_{32}; (h): Present model for ω_{32}.

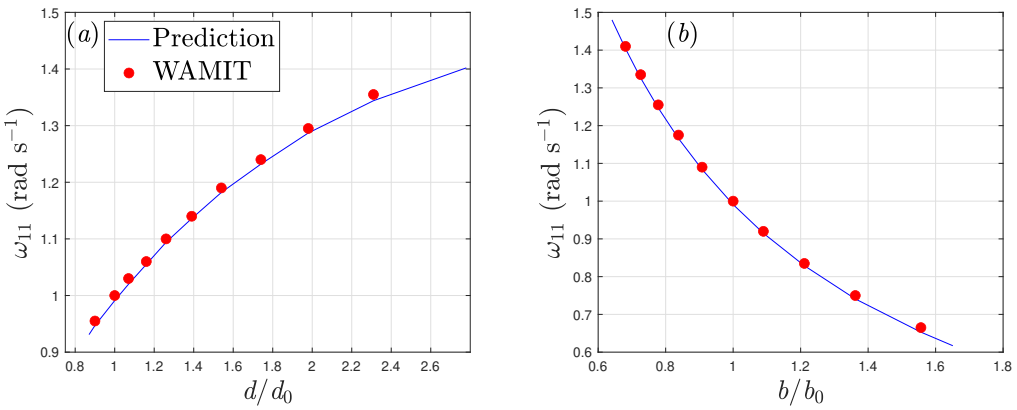

Figure 6: Variation of ω_{11} with the main dimensions of the dock. (a): Dependence on the depth of the dock d; (b) Dependence on the width of the dock b.